Electronic Journal of Linear Algebra, ISSN 1081-3810
A publication of the International Linear Algebra Society
Volume 38, pp. 227-253, March 2022.

ON THE EIGENVALUES OF MATRICES WITH COMMON GERSHGORIN REGIONS*

ANNA A. DAVIS† AND PAUL F. ZACHLIN‡

Abstract. This paper is a study of the eigenvalues of a complex square matrix with one variable nondiagonal entry expressed in polar form. Changing the angle of the variable entry while leaving the radius fixed generates an algebraic curve; as does the process of fixing an angle and varying the radius. The authors refer to these two curves as *eigenvalue orbits* and *eigenvalue trajectories*, respectively. Eigenvalue orbits and trajectories are orthogonal families of curves, and eigenvalue orbits are sets of eigenvalues from matrices with identical Gershgorin regions. Algebraic and geometric properties of both types of curves are examined. Features such as poles, singularities, and foci are discussed.

Key words. Eigenvalues, Gershgorin regions, Algebraic curves, Foci

AMS subject classifications. 15A18

1. Introduction.

1.1. Matrices with common Gershgorin regions.

Let $A = [a_{jk}]$ be an $n \times n$ complex matrix. Let

$$r_j(A) := \sum_{k \neq j} |a_{jk}|,$$

denote the sum of the absolute values of the nondiagonal entries in row j. Recall that

$$\Gamma_j(A) := \{z \in \mathbb{C} : |z - a_{jj}| \leq r_j(A)\},$$

is the jth *Gershgorin disk* of A. The *Gershgorin region* of A is defined to be the union of the Gershgorin disks, i.e.,

$$\Gamma(A) := \bigcup_{1 \leq j \leq n} \Gamma_j(A).$$

It is well known that the Gershgorin region is an eigenvalue inclusion region: since each eigenvalue λ is an element of at least one disk, we have $\lambda \in \Gamma(A)$. For a thorough treatment of Gershgorin's theorem and many related results, see Richard Varga's book [12].

There are many matrices which have the same Gershgorin region, and a natural question is to identify the set of all eigenvalues for $n \times n$ matrices with the same Gershgorin region as a given complex square matrix A. The *equimodular set* for A, denoted $\Omega(A)$ is defined as

$$\Omega(A) = \{B = [b_{jk}] : b_{jj} = a_{jj} \text{ and } |b_{jk}| = |a_{jk}| \text{ for } j \neq k\}.$$

It is clear that any matrix in $\Omega(A)$ will have the same Gershgorin region as A. We use $\sigma(\Omega(A))$ to denote the set of all eigenvalues of matrices in $\Omega(A)$. Clearly $\sigma(\Omega(A))$ is contained in the Gershgorin region of A

*Received by the editors on April 9, 2021. Accepted for publication on March 15, 2022. Handling Editor: Panagiotis Psarrakos. Corresponding Author: Paul F. Zachlin

†Department of Mathematics and Computer Science, Ohio Dominican University, Columbus, OH 43219, USA (davisa@ohiodominican.edu).

‡Department of Mathematics, Lakeland Community College, Kirtland, OH 44094, USA (pzachlin@lakelandcc.edu).

Electronic Journal of Linear Algebra, ISSN 1081-3810
A publication of the International Linear Algebra Society
Volume 38, pp. 227-253, March 2022.

and is a tighter containment region for eigenvalues of A. Varga makes use of the Perron–Frobenius theory of nonnegative matrices to show that $\sigma(\Omega(A))$ is the intersection of a number of *minimal Gershgorin sets* (see [12, Theorem 4.11]).

In this paper, we work with subsets of $\Omega(A)$ by rewriting *one* of the nondiagonal entries of A in its polar form. By allowing the angle to vary, we change the eigenvalues of the matrix without changing the Gershgorin region. In addition, we study the consequences of varying the modulus of *one* nondiagonal entry.

1.2. Definition of eigenvalue orbits and trajectories. Consider a complex square matrix A with one variable entry of the form re^{ti} $(r \geq 0, t \in [0, 2\pi))$ located off of the main diagonal.

$$A = A_{j,k}(r,t) = \begin{bmatrix} a_{11} & \dots & \dots & a_{1k} & \dots & a_{1n} \\ \vdots & & & \vdots & & \vdots \\ a_{j1} & \dots & \dots & re^{ti} & \dots & a_{jn} \\ \vdots & & & \vdots & & \vdots \\ \vdots & & & \vdots & & \vdots \\ a_{n1} & \dots & \dots & a_{nk} & \dots & a_{nn} \end{bmatrix}. \tag{1.1}$$

By fixing r and varying t, we obtain a set of eigenvalues which can be plotted in the complex plane. We call the curve that is formed an *eigenvalue orbit of* A. We use the following notation:

$$r_0\text{-orbit:} \quad \mathcal{O}_{r_0} = \{\lambda \in \mathbb{C} : \lambda \text{ is an eigenvalue of } A_{j,k}(r_0, t), t \in [0, 2\pi)\}.$$

Since the diagonal entries a_{jj} of A are constants, the centers of the Gershgorin disks stay fixed, and since the modulus of the only variable entry is fixed, the radii of all disks (and, therefore, the Gershgorin region) will also be unchanged.

On the other hand, instead of fixing r and varying t, we can fix t and vary r. When we do this, we obtain a different set of eigenvalues which we call an *eigenvalue trajectory of* A. We use the following notation:

$$t_0\text{-trajectory:} \quad \mathcal{T}_{t_0} = \{\lambda \in \mathbb{C} : \lambda \text{ is an eigenvalue of } A_{j,k}(r, t_0), r \geq 0\}.$$

If we choose to fix t and vary r, then we will vary the radius of one of the Gershgorin disks, but all other Gershgorin disks remain unchanged.

Figure 1 shows a trajectory overlaid on top of several orbits for

$$C = \begin{bmatrix} 1 & 2i & 1 \\ i & -1 & 1 \\ 0 & re^{ti} & 2 \end{bmatrix}. \tag{1.2}$$

The remainder of this paper is organized as follows. In Section 2, we show that eigenvalue orbits are algebraic curves. We show that the same is true in the case of trajectories if we ignore finitely many removable discontinuities (later shown to be poles of a rational function). In Section 3, we study points in the complex plane which are significant for these curves. In particular, we study zeros, poles, and singularities. In Section 4, we show that orbits and trajectories are *circular curves* and state results concerning their foci. We conclude the paper by suggesting some possible directions for future study in Section 5.

Electronic Journal of Linear Algebra, ISSN 1081-3810
A publication of the International Linear Algebra Society
Volume 38, pp. 227-253, March 2022.

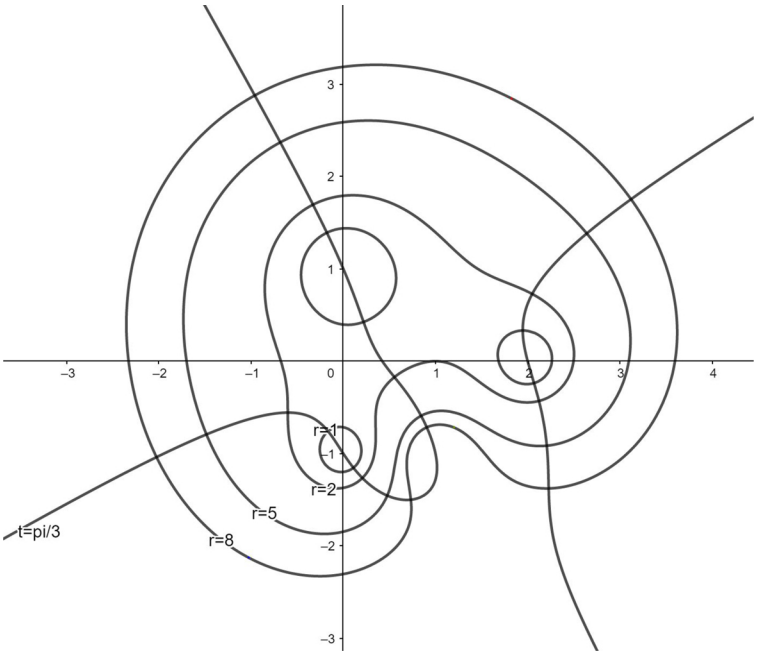

Figure 1: Orbits and a trajectory of matrix C. One orbit, such as $\mathcal{O}_1$, may consist of multiple components.

2. Equations of orbits and trajectories. Let $A = A_{j,k}(r,t)$ be an $n \times n$ matrix where the entry in row j, column k, is the variable entry re^{ti} written in polar form, as in (1.1). We compute the characteristic equation for A by expanding $\det(A - \lambda I)$ along the row (or column) containing re^{ti}. This gives us

$$p(\lambda) + re^{ti} D(\lambda) = 0, \tag{2.3}$$

where $p(\lambda)$ is some polynomial in λ, and $D(\lambda)$ is given by

$$D(\lambda) \;=\; (-1)^{j+k} \det \begin{bmatrix} a_{11} - \lambda & \dots & \dots & a_{1k} & \dots & a_{1n} \\ \vdots & & & \vdots & & \vdots \\ a_{j1} & \dots & \dots & re^{ti} & \dots & a_{jn} \\ \vdots & & & \vdots & & \vdots \\ \vdots & & & \vdots & & \vdots \\ a_{n1} & \dots & \dots & a_{nk} & \dots & a_{nn} - \lambda \end{bmatrix}$$

For an $n \times n$ matrix, the degree of $p(\lambda)$ is n. The degree of $D(\lambda)$ plays an important role in this narrative. Let

$$m = \deg\left[D(\lambda)\right].$$

Observe that $0 \le m \le n-2$.

Suppose $p(\lambda)$ and $D(\lambda)$ have no common factors. If $\lambda_0 \in \mathbb{C}$ is not a zero of $D(\lambda)$, then substituting λ_0 into (2.3) and solving for re^{ti} gives us $re^{ti} = \frac{-p(\lambda_0)}{D(\lambda_0)}$. On the other hand, if λ_0 is a zero of $D(\lambda)$, then

Electronic Journal of Linear Algebra, ISSN 1081-3810
A publication of the International Linear Algebra Society
Volume 38, pp. 227-253, March 2022.

substituting λ_0 into (2.3) yields no solutions. So, with the exception of zeros of $D(\lambda)$, every point λ_0 in the plane is an eigenvalue of some matrix $A_{j,k}(r_0, t_0)$.

Zeros of $p(\lambda)$ also play an important role. If $p(\lambda_1) = 0$, then λ_1 is an eigenvalue of A when $r = 0$. We refer to such eigenvalues as *zero-eigenvalues*.

It is easy to see that when $p(\lambda)$ and $D(\lambda)$ of (2.3) have no common factors, eigenvalue orbits defined by different values of r will be disjoint. Throughout this paper, we will continue to assume that $p(\lambda)$ and $D(\lambda)$ have no common factors. Matrix G_2 of Example 3.3 illustrates what happens when instead $p(\lambda)$ and $D(\lambda)$ have common factors. In addition, results that hold when common factors are present will be proved in a way that allows for this possibility in order to maintain the greatest possible generality.

2.1. Equation of an orbit.

THEOREM 2.1. *Let $r_0 \geq 0$. An r_0-orbit ($\mathcal{O}_{r_0}$) of an $n \times n$ matrix $A = A_{j,k}(r, t)$ is an algebraic curve given by $F(x, y) = 0$ where*

$$F(x, y) = |p(x + yi)|^2 - r_0^2 |D(x + yi)|^2, \tag{2.4}$$

is a polynomial of degree $2n$ with real coefficients.

Proof. To find $F(x, y)$, we replace λ with $x + yi$ in the characteristic equation (2.3) to obtain

$$p(x + yi) + r_0 e^{ti} D(x + yi) = 0. \tag{2.5}$$

Any $x + yi$ that satisfies (2.5) also satisfies

$$|p(x + yi)| = r_0 \, |D(x + yi)| \, ,$$

and

$$\underbrace{|p(x + yi)|^2 - r_0^2 \, |D(x + yi)|^2}_{F(x,y)} = 0. \tag{2.6}$$

Therefore, the curve $F(x, y) = 0$ contains the r_0-orbit.

To see that the r_0-orbit is equal to the curve $F(x, y) = 0$, suppose that $a + bi$ satisfies (2.6). If $D(a + bi) = 0$, then $p(a + bi) = 0$. Then $a + bi$ satisfies the characteristic equation (2.3) for all values of r, including $r = r_0$, and we have $a + bi \in \mathcal{O}_{r_0}$. On the other hand, if $D(a + bi) \neq 0$, then $a + bi$ is an eigenvalue of $A_{j,k}(R_0, t_0)$ for some $R_0 \geq 0, t_0 \in [0, 2\pi)$ determined by $R_0 e^{t_0 i} = \frac{-p(a+bi)}{D(a+bi)}$. But then $a + bi$ is an element of the R_0-orbit. As such, $a + bi$ satisfies $R_0^2 \, |D(x + yi)|^2 = |p(x + yi)|^2$. We have

$$R_0^2 = \frac{|p(a + bi)|^2}{|D(a + bi)|^2} = r_0^2.$$

Therefore, $R_0 = r_0$. We conclude that $a + bi \in \mathcal{O}_{r_0}$. ∎

COROLLARY 2.2 (Alternative Equation of an Orbit). *Let λ_ℓ ($1 \leq \ell \leq n$) be the zero-eigenvalues of an $n \times n$ matrix $A = A_{j,k}(r, t)$ and let α_ℓ ($1 \leq \ell \leq m$) be the zeros of $D(\lambda)$ in the characteristic equation (2.3). Then an r_0-orbit of A is given by*

$$\begin{aligned} 0 = |p(x + yi)|^2 - r_0^2 \, |D(x + yi)|^2 &= p(x + yi)\overline{p(x + yi)} - r_0^2 D(x + yi)\overline{D(x + yi)} \\ &= \underbrace{\prod_{n}((x + yi) - \lambda_j)((x - yi) - \bar{\lambda}_j) - r_0^2 \prod_{m}((x + yi) - \alpha_j)((x - yi) - \bar{\alpha}_j)}_{F(x,y)} . \end{aligned} \tag{2.7}$$

Electronic Journal of Linear Algebra, ISSN 1081-3810
A publication of the International Linear Algebra Society
Volume 38, pp. 227-253, March 2022.

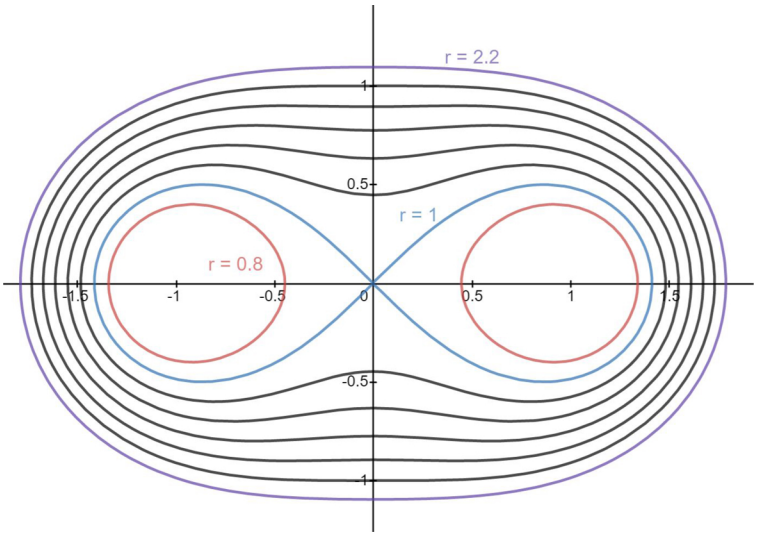

Figure 2: Orbits for the matrix $\begin{bmatrix} 1 & 1 \\ re^{ti} & -1 \end{bmatrix}$ are Cassini ovals.

For a simple illustration, consider the matrix $\begin{bmatrix} 1 & 1 \\ re^{ti} & -1 \end{bmatrix}$. The characteristic equation for this matrix is $(1-\lambda)(-1-\lambda) - re^{ti} = 0$. Using (2.6), we obtain the following equation for the orbits:

$$|1 - x - yi|^2| - 1 - x - yi|^2 - r^2 = 0, \tag{2.8}$$

or

$$(x^2 - y^2 - 1)^2 + 4x^2y^2 - r^2 = 0.$$

Considering (2.8) from a geometric standpoint, we can interpret each orbit as a collection of points $x+yi$ such that the product of distances $d(x+yi, 1)$ and $d(x+yi, -1)$ is constant:

$$d(x + yi, 1) \cdot d(x + yi, -1) = r. \tag{2.9}$$

Figures satisfying this definition are known as *Cassini ovals*. Figure 2 shows orbits for several values of r. If $0 < r < 1$, our orbit consists of two components, while we have a single closed curve for $r \geq 1$. The case $r = 1$ is special, as it contains a singularity (a node) at the origin. This famous curve is the *lemniscate of Bernoulli* (see [9] for interesting facts about this curve). We will explore the importance of orbits with singularities such as this one in Section 3.2.

2.2. Equation of a trajectory.

THEOREM 2.3. *Let $t_0 \in [0, 2\pi)$. A t_0-trajectory ($\mathcal{T}_{t_0}$) of an $n \times n$ matrix $A = A_{j,k}(r,t)$ is contained in an algebraic curve given by $G(x,y) = 0$ where*

$$G(x,y) = \left[Re\left(p(x+yi)\overline{D(x+yi)}\right)\right]\sin t_0 - \left[Im\left(p(x+yi)\overline{D(x+yi)}\right)\right]\cos t_0, \tag{2.10}$$

is a polynomial of degree $n+m$ with real coefficients.

Electronic Journal of Linear Algebra, ISSN 1081-3810
A publication of the International Linear Algebra Society
Volume 38, pp. 227-253, March 2022.

Proof. We begin by replacing λ with $x+yi$ in the characteristic equation (2.3), and proceed under the assumption that $D(x+yi) \neq 0$ (which implies that $\overline{D(x+yi)} \neq 0$).

$$p(x+yi) + re^{t_0 i} D(x+yi) = 0.$$

Subtracting $p(x+yi)$ from both sides and multiplying both sides by $\overline{D(x+yi)}$ gives us

$$\left(rD(x+yi)\overline{D(x+yi)}\right) e^{t_0 i} = -p(x+yi)\overline{D(x+yi)}, \tag{2.11}$$

This gives us

$$\begin{cases} \left(rD(x+yi)\overline{D(x+yi)}\right)\cos t_0 = \operatorname{Re}\left(-p(x+yi)\overline{D(x+yi)}\right) \\ \left(rD(x+yi)\overline{D(x+yi)}\right)\sin t_0 = \operatorname{Im}\left(-p(x+yi)\overline{D(x+yi)}\right) \end{cases}. \tag{2.12}$$

Solving each equation in (2.12) for $rD(x+yi)\overline{D(x+yi)}$ and setting the two right sides equal to each other, we obtain

$$\underbrace{\left[\operatorname{Re}\left(p(x+yi)\overline{D(x+yi)}\right)\right]\sin t_0 - \left[\operatorname{Im}\left(p(x+yi)\overline{D(x+yi)}\right)\right]\cos t_0}_{G(x,y)} = 0. \tag{2.13}$$

The curve $G(x,y)=0$ is algebraic, and it contains $\mathcal{T}_{t_0}$. The degree of $G(x,y)$ is $n+m$. If the degree, m, of $D(\lambda)$ is maximal (i.e. $m=n-2$), then the degree of G is $2n-2$. ∎

Zeros of $D(\lambda)$ satisfy (2.13), but as discussed earlier, they are not eigenvalues of $A_{j,k}(r,t)$ for any combination of r and t. We will find it convenient to extend our definition of a trajectory to include these (at most) $n-2$ discontinuities. Let

$$\overline{\mathcal{T}}_{t_0} = \mathcal{T}_{t_0} \cup \{\lambda_0 \,|\, D(\lambda_0) = 0\}.$$

The algebraic curve $G(x,y)=0$ is equal to $\overline{\mathcal{T}}_{t_0}$. We will use the term trajectory to refer to both $\overline{\mathcal{T}}_{t_0}$ and $\mathcal{T}_{t_0}$, and use notation to avoid ambiguity. Zeros of D have important geometric and algebraic properties. These will be discussed in Sections 3.1 and 4.6.

Corollary 2.4 (Alternative Equation for a Trajectory). *Let λ_ℓ $(1 \leq \ell \leq n)$ be the zero-eigenvalues of an $n \times n$ matrix $A = A_{j,k}(r,t)$ and let α_ℓ $(1 \leq \ell \leq m)$ be the zeros of $D(\lambda)$ in the characteristic equation (2.3). Then a t_0-trajectory ($\overline{\mathcal{T}}_{t_0}$) of A is given by*

$$\begin{aligned} 0 &= p(x+yi)\overline{D(x+yi)} - \overline{p(x+yi)}D(x+yi)e^{2t_0 i} \\ &= \underbrace{\prod^{n}((x+yi)-\lambda_j)\prod^{m}((x-yi)-\bar{\alpha}_j) + e^{2t_0 i}\prod^{n}((x-yi)-\bar{\lambda}_j)\prod^{m}((x+yi)-\alpha_j)}_{G(x,y)}. \end{aligned} \tag{2.14}$$

Proof. Using the identities $\operatorname{Re}(z) = \frac{z+\bar{z}}{2}$ and $\operatorname{Im}(z) = \frac{z-\bar{z}}{2i}$, we can show that (2.13) is equivalent to

$$\bar{K}p(x+yi)\overline{D(x+yi)} - K\overline{p(x+yi)}D(x+yi) = 0, \tag{2.15}$$

where $K = \cos t_0 + i \sin t_0$. To simplify further, observe that

$$\begin{aligned} \frac{K}{\bar{K}} = K^2 &= \cos^2 t_0 + 2i \sin t_0 \cos t_0 - \sin^2 t_0 \\ &= \cos(2t_0) + i\sin(2t_0) \\ &= e^{2t_0 i}. \end{aligned}$$

Electronic Journal of Linear Algebra, ISSN 1081-3810
A publication of the International Linear Algebra Society
Volume 38, pp. 227-253, March 2022.

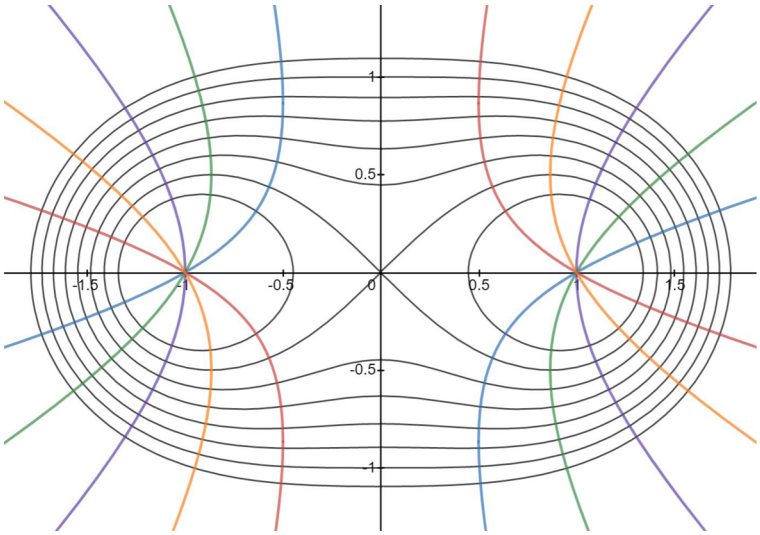

Figure 3: Trajectories for the matrix $\begin{bmatrix} 1 & 1 \\ re^{ti} & -1 \end{bmatrix}$ are hyperbolas.

The result follows from the properties of complex conjugates. ∎

Returning to the the matrix $\begin{bmatrix} 1 & 1 \\ re^{ti} & -1 \end{bmatrix}$ of Figure 2, we find that trajectories are hyperbolas given by

$$(x^2 - y^2 - 1)\sin t_0 - (2xy)\cos t_0 = 0.$$

See Figure 3.

We now give an example using a 3×3 matrix.

Example 2.5. Let

$$C = \begin{bmatrix} 1 & 2i & 1 \\ i & -1 & 1 \\ 0 & re^{ti} & 2 \end{bmatrix}.$$

The characteristic equation for C is

$$-\lambda^3 + 2\lambda^2 - \lambda + 2 + (\lambda - 1 + i)re^{ti} = 0. \tag{2.16}$$

Thus, $p(\lambda) = -\lambda^3 + 2\lambda^2 - \lambda + 2$ and $D(\lambda) = \lambda - 1 + i$. Replacing λ with $x + yi$ and using (2.13), we obtain the following equation for $\overline{\mathcal{T}}_{t_0}$

$$\begin{aligned} &\left[x^4 - 3x^3 + 3x^2y + 3x^2 - y^4 - y^3 + xy^2 - y^2 - 4xy - 3x + y + 2\right]\sin t_0 \\ &= \left[2x^3y - x^3 - 5x^2y + 2x^2 + 2xy^3 - y^3 + 3xy^2 - 2y^2 + 4xy - x + y + 2\right]\cos t_0. \end{aligned}$$

Note that $\lambda = 1 - i$ is a zero of $D(\lambda) = \lambda - 1 + i$ but is not a zero of $p(\lambda) = -\lambda^3 + 2\lambda^2 - \lambda + 2$. Thus, $\lambda = 1 - i$ is the only complex number that is never an eigenvalue of C. We will later see that *every* eigenvalue trajectory $\overline{\mathcal{T}}_{t_0}$ of matrix C passes through $1 - i$. Figure 4 shows several orbits and trajectories for C.

Electronic Journal of Linear Algebra, ISSN 1081-3810
A publication of the International Linear Algebra Society
Volume 38, pp. 227-253, March 2022.

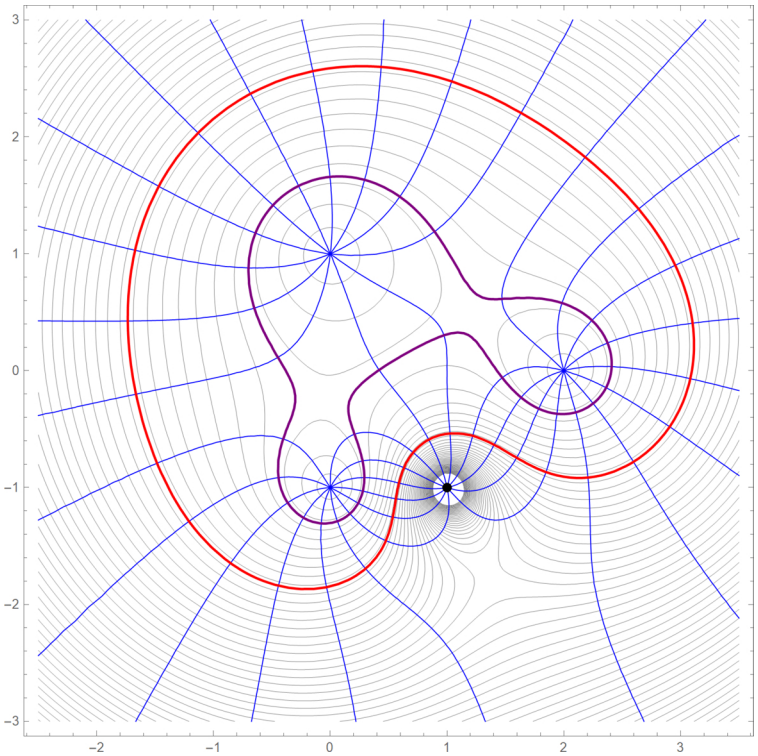

Figure 4: Orbits and trajectories for matrix C. Sample orbits $\mathcal{O}_5$ (red) and $\mathcal{O}_{1.6}$ (purple) are shown. The complex number $1-i$ is not an eigenvalue of C for any combination of r and t.

3. Special points to consider. In this section, we examine points in the complex plane that are not eigenvalues of $A_{j,k}(r,t)$, such as $1-i$ in Example 2.5. We also study singularities such as the node of the lemniscate of Bernoulli mentioned in Section 2.1. To do this, we will need an alternative way of looking at the characteristic equation (2.3). Solving equation (2.3) for re^{ti} gives us the rational function

$$re^{ti} = f(\lambda) = \frac{-p(\lambda)}{D(\lambda)}. \tag{3.17}$$

Observe that $f : \mathbb{C} \setminus \{\lambda_0 : D(\lambda_0) = 0\} \to \mathbb{C}$ maps every $\mathcal{O}_{r_0}$ to a circle of radius r_0 centered at the origin, and every trajectory $\mathcal{T}_{t_0}$ to a line through the origin determined by the angle t_0.

3.1. Zeros and poles. Under the assumption that $p(\lambda)$ and $D(\lambda)$ in 3.17 have no common factors, we immediately make the following observations:

1. Zeros of $f(\lambda)$ are the zero-eigenvalues of $A_{jk}(r,t)$.
2. Zeros of $D(\lambda)$ are the poles of $f(\lambda)$.

For every matrix $A_{jk}(r,t)$, there will be at most n distinct zero-eigenvalues and at most $n-2$ distinct poles. Because zeros of $p(\lambda)$ and $D(\lambda)$ satisfy (2.13), we have the following result.

THEOREM 3.1. *Every trajectory $\overline{\mathcal{T}}_{t_0}$ contains every zero-eigenvalue and every pole.*

Electronic Journal of Linear Algebra, ISSN 1081-3810
A publication of the International Linear Algebra Society
Volume 38, pp. 227-253, March 2022.

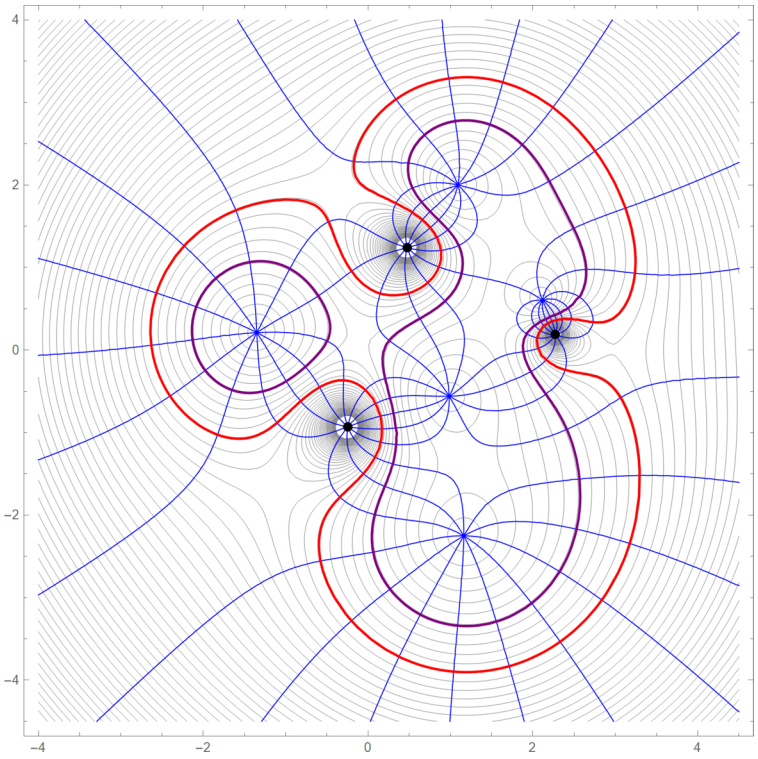

Figure 5: Orbits and trajectories for a 5×5 matrix H. Sample orbits $\mathcal{O}_5$ (red) and $\mathcal{O}_3$ (purple) are shown. There are five zero-eigenvalues and three poles.

As an illustration, consider the 5×5 matrix

$$H = \begin{bmatrix} 1 & -1 & 1-i & 2+i & 1 \\ 1 & -i & i & re^{ti} & 1+2i \\ 0 & -1 & 2 & -2 & 1-i \\ 1 & -2 & 1 & i & 1 \\ i & i-1 & 1 & 1+i & 1 \end{bmatrix}. \tag{3.18}$$

Figure 5 shows orbits and trajectories for H. Zero-eigenvalues appear as blue dots, where multiple trajectories intersect, while poles appear as black dots.

3.2. Singularities. Singularities will play an important role in determining the location of the foci of orbits. For our purposes, singularities fall into two broad categories: cusps and self-intersections. We have already encountered a singularity in the orbit of a two-by-two matrix: the node of the lemniscate of Bernoulli.

Recall that $f : \mathbb{C} \setminus \{\lambda_0 : D(\lambda_0) = 0\} \to \mathbb{C}$ of (3.17) maps every $\mathcal{O}_{r_0}$ to a circle of radius r_0 centered at the origin. Function f is analytic on its domain. Therefore, f is locally invertible at every point in its domain where $f'(\lambda) \neq 0$. Locally, f and f^{-1} are holomorphic bijections between parts of circles and parts of orbits. Because both maps are locally conformal [15, Theorem 1, p. 494], we can rule out the possibility of

Electronic Journal of Linear Algebra, ISSN 1081-3810
A publication of the International Linear Algebra Society
Volume 38, pp. 227-253, March 2022.

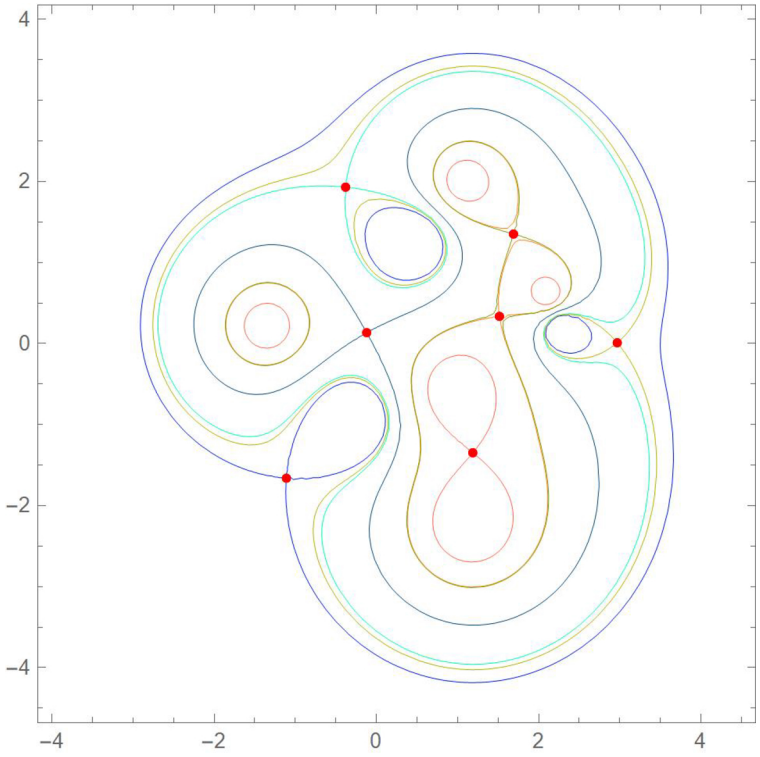

Figure 6: Singularities of orbits of H.

orbits having cusps. Therefore, the only possible type of singularity an orbit can have is a self-intersection at a point where f locally fails to be one to one [15, Theorem 2, p. 505]. We can find the location of such singularities by solving

$$f'(\lambda) = \frac{p(\lambda)D'(\lambda) - p'(\lambda)D(\lambda)}{D(\lambda)^2} = 0,$$

or equivalently,

$$p'(\lambda)D(\lambda) - p(\lambda)D'(\lambda) = 0. \tag{3.19}$$

If the degree of $p(\lambda)$ is n and the degree of $D(\lambda)$ is m, then the degree of the polynomial in (3.19) is $n+m-1$. If m is maximal, then orbits of A have $2n-3$ singularities (including multiplicity). Figure 6 shows seven orbit singularities for the 5×5 matrix H from (3.18).

As Theorem 3.2 below shows, orbit singularities correspond to eigenvalues of multiplicity greater than one.

THEOREM 3.2. *Let λ_0 be an eigenvalue of $A_{jk}(r_0, t_0)$. Orbit $\mathcal{O}_{r_0}$ has a singularity at λ_0 if and only if the multiplicity of λ_0 is greater than* 1.

Proof. Suppose the multiplicity of λ_0 is greater than 1. Then the characteristic polynomial

$$Q(\lambda) = p(\lambda) + D(\lambda)r_0 e^{t_0 i},$$

Electronic Journal of Linear Algebra, ISSN 1081-3810
A publication of the International Linear Algebra Society
Volume 38, pp. 227-253, March 2022.

has a repeated factor $(\lambda - \lambda_0)$. It is easy to see that $(\lambda - \lambda_0)$ is also a factor of $Q'(\lambda) = p'(\lambda) + D'(\lambda)r_0e^{t_0 i}$. Therefore

$$Q(\lambda_0) = p(\lambda_0) + D(\lambda_0)r_0e^{t_0 i} = 0 \quad \text{and} \quad Q'(\lambda_0) = p'(\lambda) + D'(\lambda_0)r_0e^{t_0 i} = 0.$$

Solving both equations for $r_0e^{t_0 i}$ and equating the results gives us

$$\frac{p(\lambda_0)}{D(\lambda_0)} = \frac{p'(\lambda_0)}{D'(\lambda_0)}.$$

But this is equivalent to (3.19). We conclude that λ_0 is an orbit singularity.

Conversely, suppose that λ_0 satisfies (3.19). Then

$$\frac{p(\lambda_0)}{D(\lambda_0)} = \frac{p'(\lambda_0)}{D'(\lambda_0)} = -r_0e^{t_0 i}.$$

But then

$$Q(\lambda) = p(\lambda) + D(\lambda)r_0e^{t_0 i} = 0 \quad \text{and} \quad Q'(\lambda) = p'(\lambda) + D'(\lambda)r_0e^{t_0 i} = 0.$$

Therefore, $Q(\lambda) = (\lambda - \lambda_0)q(\lambda)$ and $Q'(\lambda) = q(\lambda) + (\lambda - \lambda_0)q'(\lambda)$ for some polynomial $q(\lambda)$. But $Q'(\lambda_0) = 0$, so $Q'(\lambda_0) = q(\lambda_0) = 0$. We conclude that $(\lambda - \lambda_0)$ is a factor of $q(\lambda)$. Therefore, $(\lambda - \lambda_0)$ is a factor of $Q(\lambda)$ of multiplicity greater than 1. ∎

3.3. Orthogonality. Figures 1, 3, 4, and 5 suggest that orbits and trajectories form orthogonal families of curves. This is indeed the case. As noted earlier, function f of (3.17) maps orbits to circles centered at the origin, and trajectories to lines through the origin. Function f is conformal at every point in its domain where $f'(\lambda) \neq 0$ [15]. Combining these observations with the fact that radii are orthogonal to circles allows us to conclude that, with the exception of singularities, orbits, and trajectories are orthogonal.

3.4. Typical and not-so-typical behavior of eigenvalues. At the beginning of Section 3.1, we assumed that $p(\lambda)$ and $D(\lambda)$ have no common factors. When this is the case, and when $\deg[D(\lambda)] = m = n - 2$, and neither $p(\lambda)$ nor $D(\lambda)$ have repeated factors, orbits, and eigenvalues exhibit *typical* behavior. In this section, we describe *typical* behavior, and then give examples of what happens when one of the above conditions is not satisfied.

Consider the eigenvalues of $A_{jk}(r, t)$. When $r = 0$, the orbit consists of n zero-eigenvalues. By making r a very small positive number, we obtain n small, disjoint components of an orbit. As r increases, components grow and merge. As r continues to increase, we will observe smaller components breaking off and remaining inside one large, outer component. For a fixed, large r_0 we observe the following behavior:

1. As t varies, two eigenvalues travel around the outer component of the r_0-orbit.
2. The interior of the outer component contains $n - 2$ eigenvalues belonging to $n - 2$ disjoint orbit components.
3. Each of the $n-2$ eigenvalues located inside the outer component is orbiting a pole, getting arbitrarily close to it as r increases.

This behavior is illustrated in Figure 7 using the matrix

$$G = \begin{bmatrix} -1 & -1 & 2+i & 2 \\ 2 & -2 & re^{ti} & i-1 \\ 2-i & 3 & 2 & -1 \\ 0 & -1-i & -1 & 1 \end{bmatrix}.$$

Electronic Journal of Linear Algebra, ISSN 1081-3810
A publication of the International Linear Algebra Society
Volume 38, pp. 227-253, March 2022.

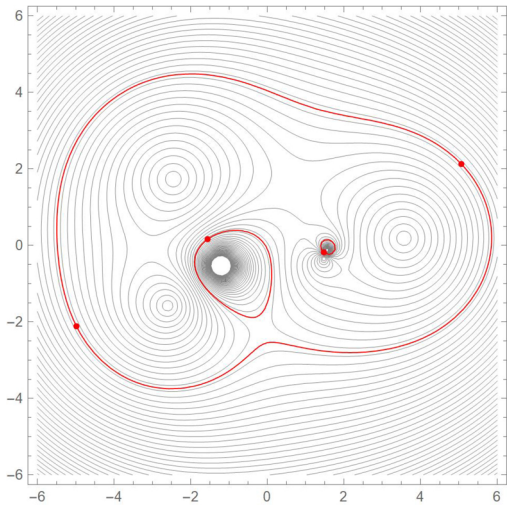

Figure 7: Typical behavior of eigenvalues is illustrated using matrix G. $\mathcal{O}_8$ is shown in red along with four eigenvalues corresponding to $t = \pi/3$. In general, for a sufficiently large value of r, two eigenvalues are located on the outer component of the orbit, while the remaining eigenvalues orbit the poles.

Now we turn our attention to some less typical behaviors.

EXAMPLE 3.3. Consider three matrices:

$$G_1 = \begin{bmatrix} 1 & -1 & 2+i & 0 \\ 0 & -2 & re^{ti} & i-1 \\ -i & 0 & 2 & -1 \\ i+1 & -1 & 0 & 2 \end{bmatrix} \quad G_2 = \begin{bmatrix} 1 & re^{ti} & -i \\ 1 & 3+2i & 2 \\ i & 0 & 3+4i \end{bmatrix} \quad G_3 = \begin{bmatrix} 1 & 0 & 2+i & 0 \\ 0 & -2 & re^{ti} & i-1 \\ -i & 1 & 2 & 0 \\ i+1 & -1 & 0 & 1 \end{bmatrix}.$$

Each of these matrices illustrates what happens when a matrix is not *typical*.

1. In the characteristic polynomial (2.3) of G_1 the degree of $D(\lambda)$ is 1, which is less than its maximum possible degree of 2. Figure 8(a) shows an eigenvalue orbiting a single pole, while three eigenvalues are located along the outer orbit.
2. In the characteristic polynomial of G_2, $p(\lambda)$ and $D(\lambda)$ have a common factor. As a result, the orbits for G_2 reduce to orbits for a 2×2 matrix, with a single fixed eigenvalue located at the zero of the common factor.
3. G_3 shows what happens when $D(\lambda)$ has repeated factors. A factor of $D(\lambda)$ of multiplicity two produces a pole that has two eigenvalues circling it. See Figure 8(b).

4. Shifting our focus to foci. Gershgorin regions are one of many well-studied eigenvalue inclusion regions. Another eigenvalue inclusion region is the *numerical range* (also known as the *field of values*) of a matrix (see Chapter 1 of [4] for a nice introduction), which is easily approximated using Johnson's method [5]. The boundary of the numerical range is the convex hull of a certain algebraic curve, as proved by Kippenhahn in [7] (see also [16] for a translation into English). Kippenhahn called this algebraic curve the *randerzeugende*, and he proved that the eigenvalues of the matrix are, in fact, the foci of the *randerzeugende*.

Electronic Journal of Linear Algebra, ISSN 1081-3810
A publication of the International Linear Algebra Society
Volume 38, pp. 227-253, March 2022.

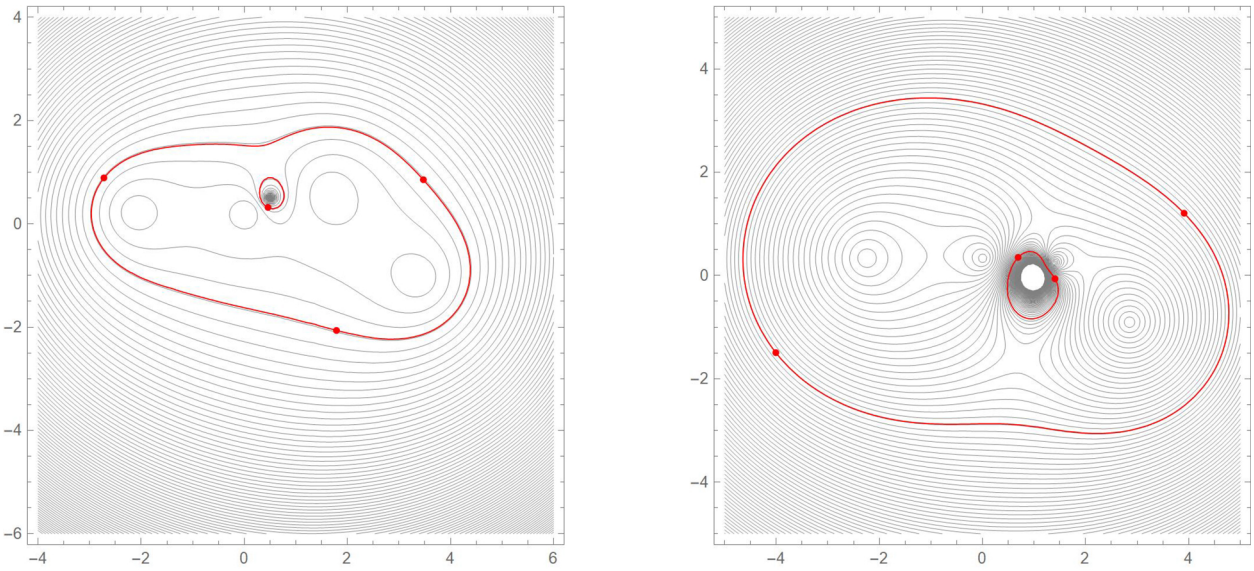

(a) An orbit with four eigenvalues of G_1.

(b) An orbit with four eigenvalues of G_3.

Figure 8: Orbits of G_1 and G_3.

From this perspective, the Gershgorin region, the numerical range, and other eigenvalue inclusion regions are regions that contain foci of the *randerzeugende*. Eigenvalue orbits and trajectories are the paths followed by these foci as we vary an entry of the matrix. We have seen that each of these paths is an algebraic curve. These curves also have foci, so it is natural to ask what we can say about the foci of orbits and trajectories. We will see that the answer has to do with the orbits containing singularities we studied in Section 3.2.

In this section, we study the foci of eigenvalue orbits and eigenvalue trajectories. If we take Kippenhahn's perspective that eigenvalues are simply the foci of the *randerzeugende* of a matrix, then we can say that we are studying the *foci of the foci*.

4.1. Foci of algebraic curves. Here we review some well-known facts about the foci of algebraic curves. An excellent introduction to foci can be found in [10]. For a more thorough treatment of what is known about foci, see [8].

Up to this point, we have considered orbits and trajectories as algebraic curves in the plane (either $\mathbb{R}^2$ or $\mathbb{C}$). Now we need to expand the setting in order to talk about the *foci* of an algebraic curve. If x and y are allowed to be complex, then (x, y) is a point in $\mathbb{C}^2$. Furthermore, there is a natural embedding of $\mathbb{C}^2$ into complex projective space, $P^2(\mathbb{C})$, where we think of (x, y) as a point with homogeneous coordinates $[X, Y, W]$, $W \neq 0$, by identifying (x, y) with $(X/W, Y/W)$. Complex projective space is the setting we desire in order to understand the foci of an algebraic curve.

Complex projective space, $P^2(\mathbb{C})$, contains a *line at infinity* with equation $W = 0$. Two points on this line, $I = [1, -i, 0]$ and $J = [1, i, 0]$, are called *circular points* at infinity. To understand the origin of this name, consider any circle $(x - a)^2 + (y - b)^2 - r^2 = 0$. Homogenization yields the equation $(X - aW)^2 + (Y - bW)^2 - r^2W^2 = 0$. Points I and J satisfy this equation.

Electronic Journal of Linear Algebra, ISSN 1081-3810
A publication of the International Linear Algebra Society
Volume 38, pp. 227-253, March 2022.

DEFINITION 4.1. *Given an algebraic curve C in the plane, the point of intersection of a tangent line to C through point I with a tangent line to C through point J is called an* ordinary focus.

DEFINITION 4.2. *If an algebraic plane curve C passes through points I and J, then the point of intersection of lines tangent to C at I and J is called a* singular focus.

To find the points of intersection of tangents to our algebraic curves (orbits and trajectories), we will use the method described by Wampler in [13]. This method makes use of *isotropic coordinates*.

4.2. Isotropic coordinates. Let $z = x + yi$ and $\overline{z} = x - yi$. If $x, y \in \mathbb{R}$, then z and $\overline{z}$ are complex conjugates. Since we are now considering points $(x, y) \in \mathbb{C}^2$, z and $\overline{z}$ cannot be assumed to be complex conjugates.

A point in $\mathbb{C}^2$ can be described using *isotropic coordinates* $(z, \overline{z}) = (x + yi, x - yi)$. The transformation of $h(x, y)$ to isotropic coordinates is accomplished by

$$\hat{h}(z, \overline{z}) = h\left(\frac{z + \overline{z}}{2}, \frac{z - \overline{z}}{2i}\right).$$

In the case of orbits and trajectories, the transformation of $F(x, y)$ and $G(x, y)$ to isotropic coordinates is easily done by replacing $x + yi$ and $x - yi$ in (2.7) and (2.14) with z and $\overline{z}$.

$$\hat{F}(z, \bar{z}) = \prod^{n}(z - \lambda_j)(\bar{z} - \bar{\lambda}_j) - r_0^2 \prod^{m}(z - \alpha_j)(\bar{z} - \bar{\alpha}_j), \tag{4.20}$$

$$\hat{G}(z, \bar{z}) = \prod^{n}(z - \lambda_j) \prod^{m}(\bar{z} - \bar{\alpha}_j) + e^{2t_0 i} \prod^{n}(\bar{z} - \bar{\lambda}_j) \prod^{m}(z - \alpha_j). \tag{4.21}$$

Where λ_l, $1 \leq l \leq n$, are the zero-eigenvalues of A and α_l, $1 \leq l \leq m$, are the zeros of $D(x + yi)$.

One-homogenization of the plane in isotropic coordinates results in points of the form $[Z, \overline{Z}, W] \in P^2(\mathbb{C})$ where $(z, \overline{z})$ is identified with $(Z/W, \overline{Z}/W)$, $W \neq 0$. It is worth noting that in isotropic coordinates $I = [1, 0, 0]$ and $J = [0, 1, 0]$.

4.3. Finding ordinary foci. Consider an algebraic curve C given by $\hat{h}(z, \bar{z}) = 0$. If a line through the circular point I is tangent to C at $(z_I, \bar{z}_I)$, then

$$\hat{h}(z_I, \bar{z}_I) = 0. \tag{4.22}$$

The equation of the tangent line has the form:

$$\hat{h}_z(z_I, \bar{z}_I)(z - z_I) + \hat{h}_{\bar{z}}(z_I, \bar{z}_I)(\bar{z} - \bar{z}_I) = 0. \tag{4.23}$$

Homogenizing the equation of the tangent line gives us

$$\hat{h}_z(z_I, \bar{z}_I)(Z - z_I W) + \hat{h}_{\bar{z}}(z_I, \bar{z}_I)(\bar{Z} - \bar{z}_I W) = 0. \tag{4.24}$$

Circular point I has isotropic coordinates $[1, 0, 0]$. Substituting I into (4.24) gives us

$$\hat{h}_z(z_I, \bar{z}_I) = 0. \tag{4.25}$$

Electronic Journal of Linear Algebra, ISSN 1081-3810
A publication of the International Linear Algebra Society
Volume 38, pp. 227-253, March 2022.

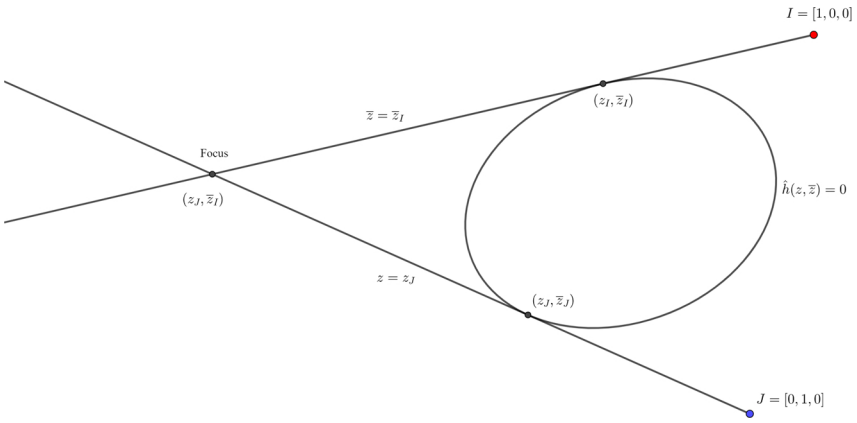

Figure 9: Point $(z_J, \bar{z}_I)$ is a focus of the curve $\hat{h}(z, \bar{z}) = 0$.

Taking (4.22) and (4.25) together, we know that $(z_I, \bar{z}_I)$ must satisfy the system

$$\begin{cases} \hat{h}_z(z, \bar{z}) = 0 \\ \\ \hat{h}(z, \bar{z}) = 0 \end{cases}.$$

Combining (4.23) and (4.25) yields the equation of the tangent line to C through I:

$$\bar{z} = \bar{z}_I.$$

A similar argument can be used to show that a line through J tangent to C at $(z_J, \bar{z}_J)$ has the equation

$$z = z_J.$$

The two tangent lines intersect at $(z_J, \bar{z}_I)$. Figure 9 summarizes this information.

Since we are only interested in finding foci with real coordinates, we will look for $(z_J, \bar{z}_I)$ such that

$$z_J = (\bar{z}_I)^*, \tag{4.26}$$

where * denotes the complex conjugate. Therefore, for our purposes, it will be sufficient to find $\bar{z}_I$ only.

4.4. Ordinary foci of orbits and trajectories. The main result of this section gives the location of ordinary foci of a nonsingular orbit $\mathcal{O}_{r_0}$ of $A = A_{j,k}(r, t)$, and establishes a connection between orbit foci and singular orbits of A. Recall that an $n \times n$ matrix A has $n + m - 1$ orbit singularities, where $m = \deg D(\lambda)$. We will use $r_s e^{t_s i}$ $(1 \leq s \leq n + m - 1)$, to denote the location of each singularity (not all singularities may be distinct). The following theorem shows that a nonsingular orbit $\mathcal{O}_{r_0}$ has $(n + m - 1)n$ foci located at intersections of $\mathcal{T}_{t_s}$ and $\mathcal{O}_{r_0^2/r_s}$.

THEOREM 4.3. *Let $A = A_{j,k}(r, t)$ be an $n \times n$ matrix. Let $\mathcal{O}_{r_0}$ be a nonsingular orbit of A. Then for every orbit singularity $r_s e^{t_s}$ $(1 \leq s \leq n + m - 1)$, there are n ordinary foci of $\mathcal{O}_{r_0}$ given by the solutions of*

$$p(z) + \frac{r_0^2}{r_s} e^{t_s i} D(z) = 0.$$

Electronic Journal of Linear Algebra, ISSN 1081-3810
A publication of the International Linear Algebra Society
Volume 38, pp. 227-253, March 2022.

Proof. We will use (2.7) and (4.20) to represent orbits. To find ordinary foci of $\mathcal{O}_{r_0}$, we need to solve the system

$$\begin{cases} \hat{F}_z(z,\bar{z}) = 0 \\ \\ \hat{F}(z,\bar{z}) = 0 \end{cases}.$$

In the definition of $\hat{F}$,

$$p(z) = \prod^{n}(z-\lambda_j) \quad \text{and} \quad D(z) = \prod^{m}(z-\alpha_j),$$

are functions of z, while

$$\overline{p(z)} = \prod^{n}(\bar{z}-\bar{\lambda}_j) \quad \text{and} \quad \overline{D(z)} = \prod^{m}(\bar{z}-\bar{\alpha}_j),$$

are functions of $\bar{z}$. So, our system can be written as

$$\begin{cases} p'(z)\overline{p(z)} - r_0^2 D'(z)\overline{D(z)} = 0 \\ \\ p(z)\overline{p(z)} - r_0^2 D(z)\overline{D(z)} = 0 \end{cases}, \tag{4.27}$$

Solving both equations for r_0^2 and setting the two expressions equal to each other we obtain:

$$p'(z)D(z) = p(z)D'(z). \tag{4.28}$$

A point z satisfies this relationship if and only if it is an orbit singularity (see (3.19)). Suppose $z_s = r_s e^{t_s i}$ satisfies (4.28). We will find $\bar{z}_s$ such that $(z_s, \bar{z}_s)$ satisfies (4.27).

Substituting z_s into the second equation, we obtain

$$\begin{aligned} p(z_s)\overline{p(z)} - r_0^2 D(z_s)\overline{D(z)} &= 0 \\ \overline{p(z)} - r_0^2 \left(\frac{D(z_s)}{p(z_s)}\right)\overline{D(z)} &= 0. \end{aligned}$$

By rearranging (2.3), we have $\frac{D(z_s)}{p(z_s)} = -\frac{1}{r_s e^{t_s i}}$. Therefore, we are looking for $\bar{z}_s$ that satisfies

$$\overline{p(z)} + \frac{r_0^2}{r_s} e^{-t_s i}\overline{D(z)} = 0. \tag{4.29}$$

By (4.26), the complex conjugate of $\bar{z}_s$, denoted by $\bar{z}_s^*$, is an ordinary focus of $\mathcal{O}_{r_0}$. But $\bar{z}_s$ satisfies (4.29) if and only if $\bar{z}_s^*$ satisfies

$$p(z) + \frac{r_0^2}{r_s} e^{t_s i} D(z) = 0. \tag{4.30}$$

This proves that the ordinary foci of $\mathcal{O}_{r_0}$ are the solutions to (4.30). ∎

Consequences of Theorem 4.3:

1. Observe that (4.30) has the form (2.3) of a characteristic equation of $A_{jk}(r,t)$ where $r = \frac{r_0^2}{r_s}$ and $t = t_s$. Therefore, ordinary foci are located along trajectories containing orbit singularities. The radii of the orbits containing ordinary foci of $\mathcal{O}_{r_0}$ are $\frac{r_0^2}{r_s}$, where each r_s is the radius of an orbit with a singularity.

Electronic Journal of Linear Algebra, ISSN 1081-3810
A publication of the International Linear Algebra Society
Volume 38, pp. 227-253, March 2022.

2. Since (4.30) is a polynomial equation of degree n and orbits of A have $n+m-1$ singularities, it follows that $\mathcal{O}_{r_0}$ has $(n+m-1)n$ ordinary foci.
3. When $m = \deg D(\lambda)$ is maximal, the number of ordinary foci is $(2n-3)n$.

THEOREM 4.4. *Let $A = A_{j,k}(r,t)$ be an $n \times n$ matrix. Let $\overline{\mathcal{T}}_{t_0}$ be a nonsingular trajectory of A. Then for every orbit singularity $r_s e^{t_s}$ $(1 \le s \le n+m-1)$, there are n ordinary foci of $\overline{\mathcal{T}}_{t_0}$ given by the solutions of*

$$p(z) + r_s e^{(2t_0 - t_s)i} D(z) = 0. \tag{4.31}$$

Proof. We apply the method used to prove Theorem 4.3 to equation (4.21). ∎

Consequences of Theorem 4.4:

1. Observe that (4.31) has the form (2.3) of a characteristic equation of $A_{jk}(r,t)$ where $r = r_s$ and $t = 2t_0 - t_s$. We conclude that the foci of $\overline{\mathcal{T}}_{t_0}$ are located on $\mathcal{O}_{r_s}$.
2. Since (4.31) is a polynomial equation of degree n and orbits of A have $n+m-1$ singularities, $\overline{\mathcal{T}}_{t_0}$ has $(n+m-1)n$ ordinary foci – same as the number of ordinary foci for an orbit.
3. When $m = \deg D(\lambda)$ is maximal, the number of ordinary foci is $(2n-3)n$.

4.5. Circularity of orbits and trajectories. Points $J = [1, i, 0]$ and $I = [1, -i, 0]$ are called circular because every homogenized circle passes through them. Algebraic curves that contain the circular points are called *circular*. A singularity is said to have order n if all partial derivatives through order $n-1$ vanish at that point. If an algebraic curve has a singularity of order n at a circular point then the curve is called *n-circular*.

Consider an algebraic curve of degree $2n$ given by $h(x,y) = 0$. We can express h as a sum $h = h_{2n} + h_{2n-1} + \cdots + h_1 + h_0$, where each h_j is a homogeneous polynomial of degree j. Homogenization yields $h(x,y,w) = h_{2n}(x,y) + w h_{2n-1}(x,y) + w^2 h_{2n-2}(x,y) + \cdots + w^{2n-1} h_1(x,y) + w^{2n} h_0$. To examine the circularity of $h(x,y) = 0$, we will take advantage of the fact that (x^2+y^2) vanishes at I and J. Therefore, to prove that $h(x,y) = 0$ is n-circular, it suffices to show that each h_{2n-k} is divisible by $(x^2+y^2)^{n-k}$, $0 \le k < n$.

THEOREM 4.5. *Orbits generated by an $n \times n$ matrix $A = A_{j,k}(r,t)$ are n-circular.*

Proof. Every orbit is defined by $F(x,y) = 0$, as in (2.4). We can express $F(x,y)$ as the sum $F = F_{2n} + F_{2n-1} + \cdots + F_1 + F_0$, where each F_j is a homogeneous polynomial of degree j. Our goal is to show that each F_{2n-k} is divisible by $(x^2+y^2)^{n-k}$, $0 \le k < n$. We will do this by using $\hat{F}(z,\bar{z})$ of (4.20). *Up to coefficients*, each F_{2n-k} is given by

$$\sum_{j=0}^{k} z^{n-j} \bar{z}^{n-k+j} = z^{n-k} \bar{z}^{n-k} \sum_{j=0}^{k} z^{k-j} \bar{z}^{j}.$$

Since $z\bar{z} = x^2 + y^2$, we get the desired divisibility. ∎

THEOREM 4.6. *Trajectories generated by an $n \times n$ matrix with a characteristic equation $p(\lambda) + re^{ti} D(\lambda) = 0$, have circularity equal to the degree of $D(\lambda)$.*

Proof. Let m be the degree of $D(\lambda)$. Every trajectory is defined by $G(x,y) = 0$, as in (2.14), where $G(x,y)$ is a polynomial of degree $n+m$. We can write G as a sum of homogeneous polynomials $G = G_{n+m} + G_{n+m-1} + \cdots + G_1 + G_0$, where each G_j is a homogeneous polynomial of degree j. We will show

Electronic Journal of Linear Algebra, ISSN 1081-3810
A publication of the International Linear Algebra Society
Volume 38, pp. 227-253, March 2022.

that every G_{n+m-k} is divisible by $(x^2+y^2)^{m-k}$, $0 \le k < m$. To do this, we will use $\hat{G}(z,\bar{z})$ of (4.21). *Up to coefficients*, each G_{n+m-k} is given by

$$\sum_{j=0}^{k} z^{n-j}\bar{z}^{m-(k-j)} + \sum_{j=0}^{k} z^{m-j}\bar{z}^{n-(k-j)}$$
$$= z^{m-k}\bar{z}^{m-k}\left[\sum_{j=0}^{k} z^{n-j-m+k}\bar{z}^{j} + \sum_{j=0}^{k} z^{k-j}\bar{z}^{n+j-m}\right].$$

Therefore, each G_{n+m-k} is divisible by $(z\bar{z})^{m-k} = (x^2+y^2)^{m-k}$. ∎

Recall that the maximal degree of $D(\lambda)$ for an $n \times n$ matrix is $n-2$. So, Theorem 4.6 implies that the circularity of a trajectory is at most $n-2$.

4.6. Singular foci of orbits and trajectories. Singular foci are the points of intersection of lines tangent to the curve at the circular points I and J. A curve must pass through the circular points in order to have a singular focus. Orbits for an $n \times n$ matrix are n-circular, while trajectories are m-circular, where m is the degree of $D(\lambda)$, $m \le n-2$. This means that, with the exception of trajectories of matrices for which $m = 0$ (e.g. 2×2 matrices), all orbits and trajectories have singular foci.

To find singular foci, we will perform two homogenization of the plane, as described by Wampler in [13]. In the new coordinate system points have the form $([Z,W],[\bar{Z},\bar{W}]) \in P^1(\mathbb{C}) \times P^1(\mathbb{C})$. The two homogenization of $\hat{h}(z,\bar{z})$, denoted by $H(Z,W,\bar{Z},\bar{W})$, is done by making the substitution $(z,\bar{z}) = \left(\frac{Z}{W}, \frac{\bar{Z}}{\bar{W}}\right)$ and clearing denominators.

As in Section 4.4, we use the notation $(z_J, \bar{z}_I)$ to denote singular foci. By Theorem 1 of [13], we can find $(z_J, \bar{z}_I)$ by using the fact that $([z_J,1],[1,0])$ and $([1,0],[\bar{z}_I,1])$ are roots of $H(Z,W,\bar{Z},\bar{W})$. As before, because we are only interested in real singular foci, it will be sufficient to find only one of z_J and $\bar{z}_I$.

THEOREM 4.7. *Zero-eigenvalues of $A_{j,k}(r,t)$ are the singular foci of every orbit of $A = A_{j,k}(r,t)$.*

Proof. We proceed with the two homogenization of (4.20):

$$\prod^{n}(z-\lambda_j)(\bar{z}-\bar{\lambda}_j) - r^2\prod^{m}(z-\alpha_j)(\bar{z}-\bar{\alpha}_j) = 0.$$

Making the substitution $(z,\bar{z}) = \left(\frac{Z}{W}, \frac{\bar{Z}}{\bar{W}}\right)$, we obtain

$$\prod^{n}(Z/W-\lambda_j)(\bar{Z}/\bar{W}-\bar{\lambda}_j) - r^2\prod^{m}(Z/W-\alpha_j)(\bar{Z}/\bar{W}-\bar{\alpha}_j) = 0.$$

Clearing the denominators by multiplying both sides of the equation by $W^n\bar{W}^n$ gives us

$$\prod^{n}(Z-W\lambda_j)(\bar{Z}-\bar{W}\bar{\lambda}_j) - W^{n-m}\bar{W}^{n-m}r^2\prod^{m}(Z-W\alpha_j)(\bar{Z}-\bar{W}\bar{\alpha}_j) = 0.$$

Letting $\bar{Z} = 1, W = 1, \bar{W} = 0$, and solving for Z, we obtain solutions $Z = \lambda_1, \ldots, \lambda_n$. But these are the zero-eigenvalues of A. ∎

THEOREM 4.8. *Poles of $A = A_{j,k}(r,t)$ are the singular foci of every trajectory of A.*

Electronic Journal of Linear Algebra, ISSN 1081-3810
A publication of the International Linear Algebra Society
Volume 38, pp. 227-253, March 2022.

Proof. Two homogenization (4.21) yields

$$\bar{W}^{n-m}\prod^{n}(Z-W\lambda_j)\prod^{m}(\bar{Z}-\bar{W}\bar{\alpha}_j)+W^{n-m}e^{2t_0 i}\prod^{n}(\bar{Z}-\bar{W}\bar{\lambda}_j)\prod^{m}(Z-W\alpha_j)=0.$$

Letting $\bar{Z}=1, W=1, \bar{W}=0$, and solving for Z, we find that the solutions, $Z=\alpha_1,\ldots,\alpha_m$, are the poles of A. ∎

Example 4.9. To illustrate Theorems 4.3 and 4.7, consider the matrix

$$B=\begin{bmatrix}1+i & i & 1\\ 1+i & -1 & 2\\ 2 & re^{ti} & -2i\end{bmatrix}.$$

According to Theorem 4.7, singular foci of every orbit of B are located at the zero-eigenvalues. Three distinct singular foci are shown in black in Figure 10.

According to Theorem 4.3, ordinary foci lie along trajectories that contain orbit singularities. In this case, $\deg D(\lambda)=1$ is maximal, so there are three orbit singularities whose locations can be found by solving (3.19). Let $r_1e^{t_1 i}$, $r_2e^{t_2 i}$, $r_3e^{t_3 i}$ be the three singularities of orbits of B.

Consider the orbit $\mathcal{O}_{r=2}$, shown in red in Figure 10. The foci of $\mathcal{O}_{r=2}$ can be found by solving

$$p(z)+\frac{2^2}{r_s}e^{t_s i}D(z)=0,$$

where

$$p(z)=-z^3-iz^2+2iz-(2-4i)\quad\text{and}\quad D(z)=2z-(1+i),$$

for z ($s=1,2,3$). This is a cubic equation. Three sets of three solutions produce nine ordinary foci of $\mathcal{O}_{r=2}$.

Parts (a)–(c) of Figure 10 show each of the three sets of ordinary foci. Each focus lies on $\mathcal{T}_{t_s}$ and $\mathcal{O}_{r=4/r_s}$. Figure 10(d) shows all 12 distinct foci of $\mathcal{O}_{r=2}$.

4.7. Counting foci. The number of foci (ordinary and singular) of an algebraic curve is the same as the class of the curve, d^*. The class of an algebraic curve is the degree of the dual curve. According to Plucker's formula

$$d^*=d(d-1)-2\delta-3\kappa, \tag{4.32}$$

where d is the degree of the algebraic curve, δ is the number of ordinary double points and κ is the number of cusps. Higher-order singularities are counted as combinations of double points. For example, a singularity of order K will be counted as $\frac{(K-1)K}{2}$ double points. Singular points at infinity are included in this count.

When counting foci, we need to account for multiplicity. Multiplicity of singular foci arises from a tangent line through a circular point having multiple points of contact with the tangent branch of the curve at the circular point. An arbitrary line crossing an n-circular curve at a circular point has n points of contact with the curve at the circular point. If the line in question is tangent to one of the branches, it has $n+1$ points of contact with the curve at the circular point: one with each non-tangential branch and two with the tangent branch. An intersection of two such tangent lines produces a double singular focus. For example, a circle is a 1-circular curve. Its center is a double singular focus. If the point of tangency is also an inflection point for the tangent branch, then it is counted as a triple point of contact with the tangent branch, and produces a triple focus. Higher contact counts are also possible.

Electronic Journal of Linear Algebra, ISSN 1081-3810
A publication of the International Linear Algebra Society
Volume 38, pp. 227-253, March 2022.

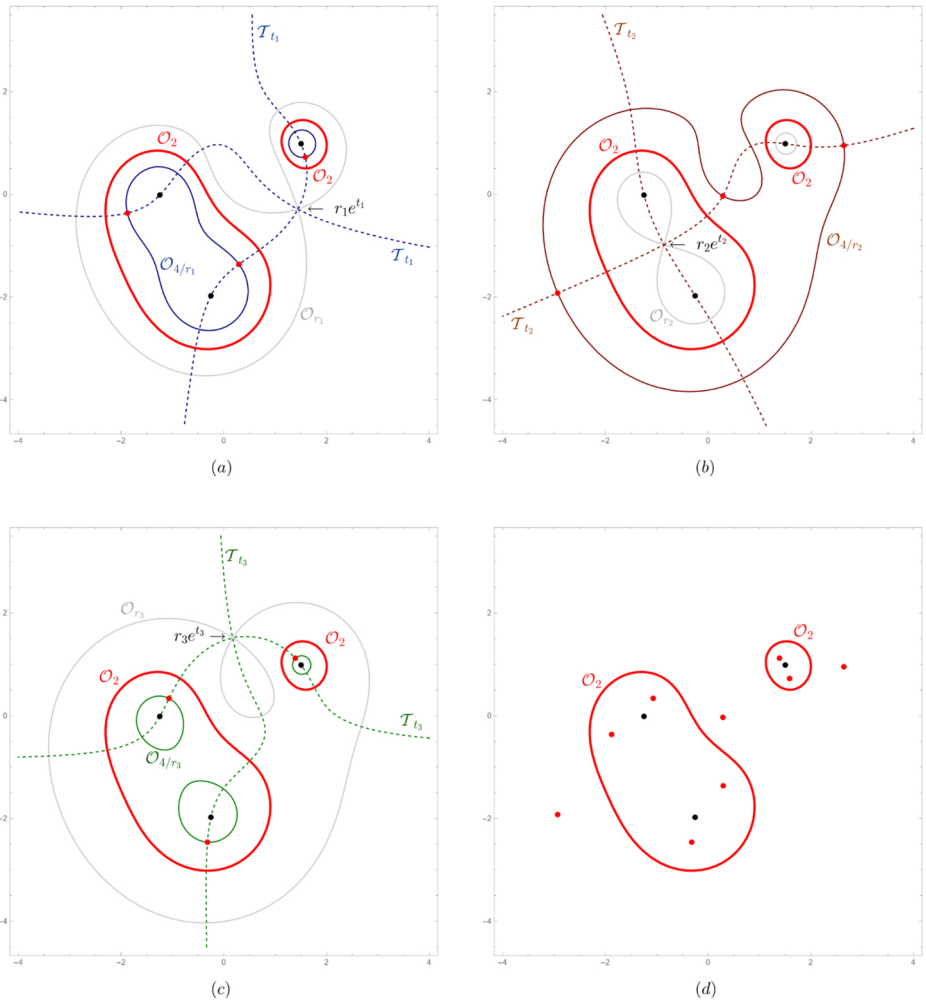

Figure 10: (a)–(c) $\mathcal{O}_2$ (red) shown together with its three singular foci (black) and three sets of ordinary foci (red). Each set of ordinary foci is located on a trajectory $\mathcal{T}_s$ containing an orbit singularity $r_s e^{t_s i}$ and belongs to the orbit whose radius is $4/r_s$. (d) $\mathcal{O}_2$ together with its twelve distinct foci.

THEOREM 4.10. *Let $A = A_{jk}(r,t)$ be an $n \times n$ matrix. Let $D(\lambda)$ be defined as in (2.3), and let $m = \deg(D(\lambda))$. Then each singular focus of the orbits of A has multiplicity*

$$n - m + 1.$$

Proof. Suppose the orbits of A each have n distinct singular foci at the n zero-eigenvalues $\lambda_1, \ldots, \lambda_n$. Consider the tangent line to an orbit at the circular point $[1, i, 0]$ passing through the singular focus λ_ℓ. The equation of such a tangent line in homogeneous coordinates is

$$X + Yi = \lambda_\ell W.$$

Electronic Journal of Linear Algebra, ISSN 1081-3810
A publication of the International Linear Algebra Society
Volume 38, pp. 227-253, March 2022.

(The equation of its counterpart through $[1,-i,0]$ is $X-Yi=\lambda_\ell W$). The degree of an orbit is $2n$, so, by Bezout's theorem, each tangent line has $2n$ points of contact with the orbit. We will find the points of contact for a tangent line at $[1,i,0]$; computations for a tangent line at $[1,-i,0]$ are identical.

Based on (4.20), we can write an equation for the orbit using homogeneous coordinates as follows:

$$\prod_{j=1}^{n}(X+Yi-\lambda_j W)(X-Yi-\bar{\lambda}_j W)-W^{2n-2m}r_0^2\prod_{j=1}^{m}(X+Yi-\alpha_j W)(X-Yi-\bar{\alpha}_j W)=0.$$

Substituting $X=\lambda_\ell W-Yi$, we obtain a polynomial equation in Y and W.

$$\underbrace{\prod_{j=1}^{n}(\lambda_\ell W-\lambda_j W)(\lambda_\ell W-2Yi-\bar{\lambda}_j W)}_{0}-W^{2n-2m}r_0^2\prod_{j=1}^{m}(X+Yi-\alpha_j W)(X-Yi-\bar{\alpha}_j W)=0$$

$$-W^{2n-2m}r_0^2\prod_{j=1}^{m}(\lambda_\ell W-\alpha_j W)(\lambda_\ell W-2Yi-\bar{\alpha}_j W)=0$$

$$W^{2n-m}\prod_{j=1}^{m}(\lambda_\ell W-2Yi-\bar{\alpha}_j W)=0.$$

This gives us m finite points of contact and $2n-m$ points of contact at $[1,i,0]$. For an n-circular curve, this means that the tangent has a single point of contact at $[1,i,0]$ with each of the nontangent branches, and $n-m+1$ points of contact with the tangent branch. ∎

As an immediate consequence of Theorem 4.10, we see that when the degree of $D(\lambda)$ is maximal (i.e. $m=n-2$), every singular focus is a triple focus. A similar argument shows that singular foci of trajectories, when m is maximal, are also triple foci. Example 4.11 illustrates what can happen when m is not maximal.

Suppose an $n\times n$ matrix A is such that $\deg D(\lambda)$ is maximal. Then for orbits and trajectories of A that have no singularities (other than those at circular points), we have the following counts:

	Degree of Curve	Circularity	Double Points at I and J
Orbits	$2n$	n	$2\cdot\frac{(n-1)n}{2}$
Trajectories	$2n-2$	$n-2$	$2\cdot\frac{(n-3)(n-2)}{2}$

Plucker's formulas give us the following number of foci for orbits and trajectories, respectively:

$$d_{\mathcal{O}}^{*}=2n(2n-1)-2\cdot 2\cdot\frac{(n-1)n}{2}=2n^2, \tag{4.33}$$

$$d_{\mathcal{T}}^{*}=(2n-2)(2n-3)-2\cdot 2\cdot\frac{(n-3)(n-2)}{2}=2n^2-6. \tag{4.34}$$

By Theorems 4.3 and 4.4, both orbits and trajectories have $(2n-3)n$ ordinary foci. Orbits have n triple singular foci at zero-eigenvalues, and trajectories have $n-2$ triple singular foci at the poles. This gives us a total of $(2n-3)n+3n=2n^2$ foci for nonsingular orbits and $(2n-3)n+3(n-2)=2n^2-6$ foci for nonsingular trajectories. These results are in agreement with (4.33) and (4.34).

The following example illustrates what can happen when m is not maximal.

Electronic Journal of Linear Algebra, ISSN 1081-3810
A publication of the International Linear Algebra Society
Volume 38, pp. 227-253, March 2022.

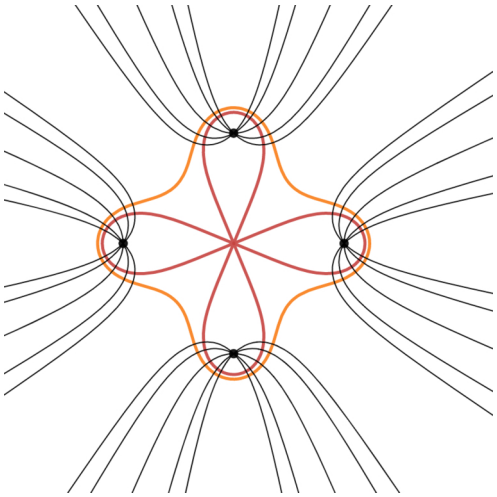

Figure 11: Singular orbit $\mathcal{O}_1$ (red) and a nonsingular orbit $\mathcal{O}_{1.3}$ (orange), together with several trajectories. All orbits have quintuple singular foci at ± 1 and $\pm i$.

Example 4.11. Consider the matrix[1]

$$M = \begin{bmatrix} 1 & 1 & 0 & 0 \\ 0 & i & 1 & 0 \\ 0 & 0 & -1 & 1 \\ re^{ti} & 0 & 0 & -i \end{bmatrix}.$$

The characteristic equation for M is

$$(1-\lambda)(i-\lambda)(-1-\lambda)(-i-\lambda) - re^{ti} = 0.$$

Note that $\deg D(\lambda) = 0$. Therefore, trajectories for M are not circular and have no singular foci.

Orbits of M have four singular foci located at ± 1 and $\pm i$. By Theorem 4.10, the multiplicity of each singular focus is $4 - 0 + 1 = 5$. This means that each orbit of M has 20 singular foci. Figure 11 shows the singular foci of orbits of M, together with two orbits and some trajectories.

It is interesting to note that orbits of M are closely related to Cassini ovals. Recall that Cassini ovals have two defining points (one at each singular focus), and the oval consists of all points for which the product of distances to the singular foci is a given constant. Orbits of M have four defining points, also located at the singular foci. In the complex plane, an orbit of M consists of all points z that satisfy the equation

$$d(z,1) \cdot d(z,i) \cdot d(z,-1) \cdot d(z,-i) = r,$$

for a fixed r. Indeed, a generalized version of ovals of Cassini can be made using orbits of $n \times n$ matrices by letting the diagonal entries be the n^{th} roots of unity, $(i, i+1)$-entries be 1, the $(n,1)$-entry be re^{ti}, and the remaining entries be 0. The 2×2 matrix that generated Cassini ovals in Figure 2 has the aforesaid form. In general, the multiplicity of each singular focus for such matrices is $n+1$.

[1]The structure of this matrix was borrowed from Varga [12, p. 106].

Electronic Journal of Linear Algebra, ISSN 1081-3810
A publication of the International Linear Algebra Society
Volume 38, pp. 227-253, March 2022.

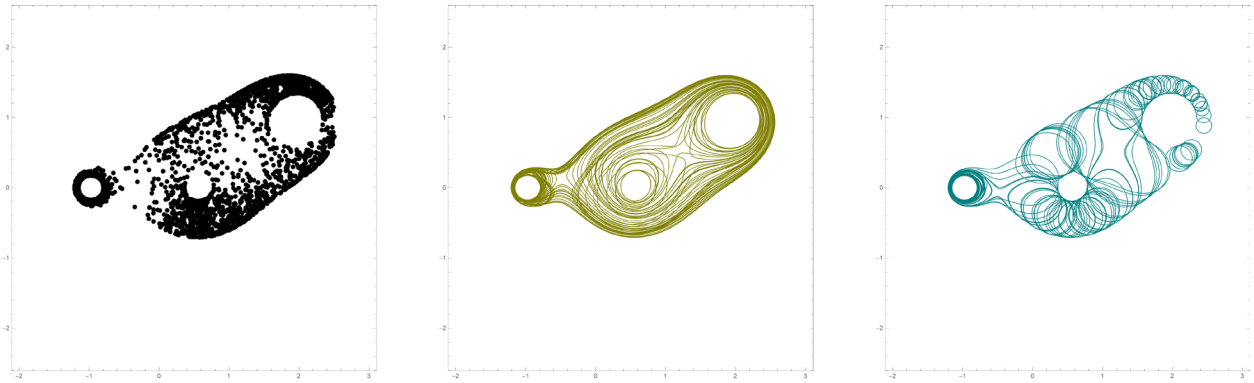

(a) Eigenvalues of 1000 elements of $\Omega(A)$.

(b) 50 orbits generated by entry (2,3).

(c) 50 orbits generated by entry (3,1).

Figure 12: Using eigenvalues versus using orbits to estimate the shape of $\sigma(\Omega(A))$.

5. Connections and possible directions for future study[2].

5.1. An application to eigenvalues of equimodular sets. In Section 1, we mentioned that Varga characterized $\sigma(\Omega(A))$ – the set of all eigenvalues of matrices in the equimodular set $\Omega(A)$ – as the intersection of a family of *minimal Gershgorin sets*.[12] Approximating $\sigma(\Omega(A))$ is a computationally difficult problem (see [2] and [3]). It is customary to estimate the shape of $\sigma(\Omega(A))$ by plotting eigenvalues of thousands of elements of $\Omega(A)$ to produce images such as the one in Figure 12(a), which shows elements of $\sigma(\Omega(A))$ for $A = \begin{bmatrix} -1 & 1 & 0 \\ 0 & 2+i & 1 \\ 1 & 1 & 0.5 \end{bmatrix}$.

Eigenvalue orbits offer an alternative way of visualizing $\sigma(\Omega(A))$, at least for small matrices. To generate orbit visualizations for $\sigma(\Omega(A))$, consider elements of $\Omega(A)$ of the form

$$\begin{bmatrix} -1 & e^{\theta_1 i} & 0 \\ 0 & 2+i & e^{ti} \\ e^{\theta_2 i} & e^{\theta_3 i} & 0.5 \end{bmatrix},$$

where entry $(2,3)$ is the orbit-generating variable entry with radius $r = a_{23} = 1$. Every random triplet $(\theta_1, \theta_2, \theta_3)$ gives rise to an eigenvalue orbit. A plot of 50 such orbits is shown in Figure 12(b). Any nondiagonal entry of A can be used as an orbit-generating entry with radius $r = a_{jk}$. For example, if entry $(3,1)$ is used as an orbit generator, we get the image in Figure 12(c). If each of the four nonzero, nondiagonal entries of A is used as an orbit generator and the results are combined, we obtain an approximation of $\sigma(\Omega(A))$ shown in Figure 13(a).

The orbit-generating algorithm used to create graphs for this paper was written in Wolfram Mathematica, and is a direct implementation of the process for finding orbits described in this paper. As such, the algorithm involves symbolic computations, making it prohibitive for large matrices. Mathematica's `Timing[]` function

[2]The authors thank the anonymous referees for their suggestions which improved the paper, including a number of the ideas in this final section.

Electronic Journal of Linear Algebra, ISSN 1081-3810
A publication of the International Linear Algebra Society
Volume 38, pp. 227-253, March 2022.

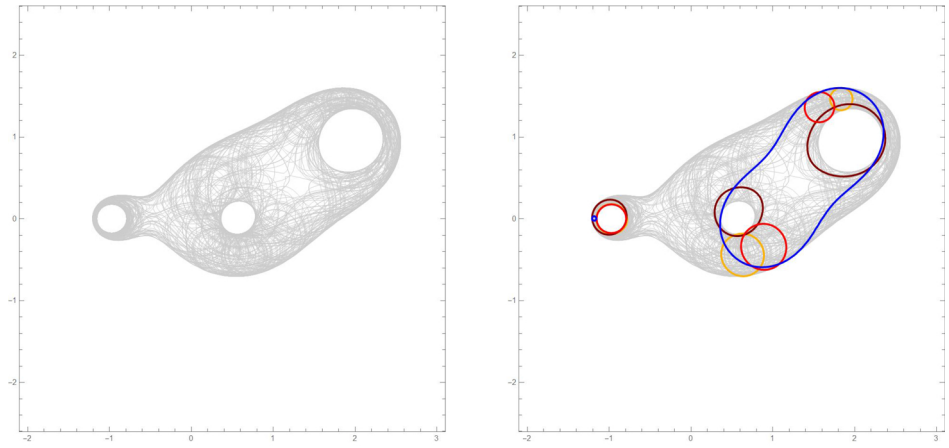

(a) Four sets of 50 orbits used to approximate the shape of $\sigma(\Omega(A))$.

(b) Estimated shape of $\sigma(\Omega(A))$ together with four additional orbits.

Figure 13: A visual exploration of relationships between $\sigma(\Omega(A))$ and individual orbits.

was used to compare the efficiency of the orbit generating algorithm with that of estimating equimodular regions by direct computation of eigenvalues. In one of the test runs, CPU time for generating orbits in Figure 13(a) was 11.73 s, while CPU time for generating eigenvalues in Figure 12a was 21.98 s.

The orbit-generating algorithm has been tested on matrices of size up through $n = 6$. The comparative advantage of the algorithm seen for $n = 3$ disappears as n increases. So, while it performs well for small values of n, the current implementation of the orbit-generating algorithm is not recommended for large matrices. The method's advantage lies not in its efficiency, but in the greater amount of detail it provides, allowing for better visual exploration. For instance, Figure 13(b), in which individual orbits appear to be tangent to the boundary of $\sigma(\Omega(A))$, suggests possible relationships between the boundary of an equimodular region and individual orbits and offers a direction for future study.

5.2. A note on varying a diagonal entry. Due to the definition of equimodular regions, the focus of this paper has been on matrices with a variable non-diagonal entry. In this section, we consider an alternative. If in Definition 1.1 we allow the variable entry re^{ti} to be located along the diagonal, we obtain a matrix $A_{jj}(r,t)$ whose characteristic equation is

$$\tilde{p}(\lambda) + re^{ti}\tilde{D}(\lambda) = 0, \tag{5.35}$$

This equation is derived by expanding along the row (or column) containing the variable entry. The new characteristic equation is identical in form to (2.3), but while $\deg(D(\lambda)) \leq n-2$, we now have $\deg\left(\tilde{D}(\lambda)\right) \leq n-1$ for an $n \times n$ matrix A.

Definitions of orbits and trajectories are still appropriate in this setting, and the corresponding results regarding equations ((2.1), (2.3)), singularities (3.19), poles, and the orthogonality property (3.3) still hold in this setting. It is interesting to note that due to $\tilde{D}(\lambda)$ having a higher degree than $D(\lambda)$, even a 2×2 matrix $A_{jj}(r,t)$ will generally have a pole. The following example illustrates all of the above properties.

Electronic Journal of Linear Algebra, ISSN 1081-3810
A publication of the International Linear Algebra Society
Volume 38, pp. 227-253, March 2022.

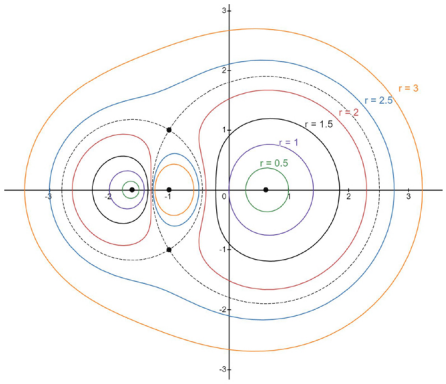

(a) Several orbits of matrix $\tilde{A}$, together with zero eigenvalues ($z = -0.5 \pm \sqrt{5}/2$), singularities ($z = -1 \pm i$) and a pole (z=-1).

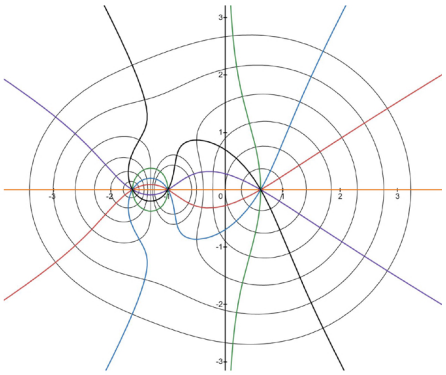

(b) Several trajectories of matrix $\tilde{A}$.

Figure 14: Orbits and trajectories of $\tilde{A}$ of Example 5.1.

EXAMPLE 5.1. Consider the matrix

$$\tilde{A} = \begin{bmatrix} re^{ti} & 1 \\ 1 & -1 \end{bmatrix}.$$

The characteristic equation of $\tilde{A}$ is $\tilde{p}(\lambda) + re^{ti}\tilde{D}(\lambda) = 0$ where

$$\tilde{p}(\lambda) = \lambda^2 + \lambda - 1, \quad \text{and} \quad \tilde{D}(\lambda) = -1 - \lambda.$$

Using (2.1) and (2.3), we find that the equations of orbits and trajectories are given, respectively, by

$$(x^2 + x - y^2 - 1)^2 + (2xy + y)^2 - r_0(1 + 2x + x^2 + y^2) = 0,$$

and

$$(-x^3 - 2x^2 - xy^2 + 1)\sin t_0 + y(x^2 + 2x + y^2 + 2)\cos t_0 = 0.$$

Zero eigenvalues are $-0.5 \pm \sqrt{5}/2$. Singularities are located at $-1 \pm i$. There is a pole at -1. See Figure 14.

5.3. Connections with pseudospectra. Let A be a nonsingular $n \times n$ matrix and let $\varepsilon > 0$. The ε-pseudospectrum is a bounded set in the complex plane defined by one of the following equivalent characterizations:

$$\begin{aligned} \Lambda_\varepsilon(A) &= \{\, z \,:\, \|(A - zI)^{-1}\| > \varepsilon^{-1} \,\} \\ &= \{\, z \,:\, \sigma_{\min}(A - zI) < \varepsilon \,\} \\ &= \{\, z \,:\, \exists\, E,\ \|E\| < \varepsilon,\ A + E - zI \text{ singular} \,\} \\ &= \{\, z \,:\, \exists\, E, v,\ \|E\| < \varepsilon,\ \|v\| = 1,\ (A + E)\, v = z\, v \,\}. \end{aligned} \tag{5.36}$$

Here $\|\cdot\|$ denotes the matrix 2-norm, with the convention that $\|(A - zI)^{-1}\| = \infty$ when z is an eigenvalue of A, and $\sigma_{\min}(A)$ denotes the minimal singular value of A. Pseudospectra give useful information on the

Electronic Journal of Linear Algebra, ISSN 1081-3810
A publication of the International Linear Algebra Society
Volume 38, pp. 227-253, March 2022.

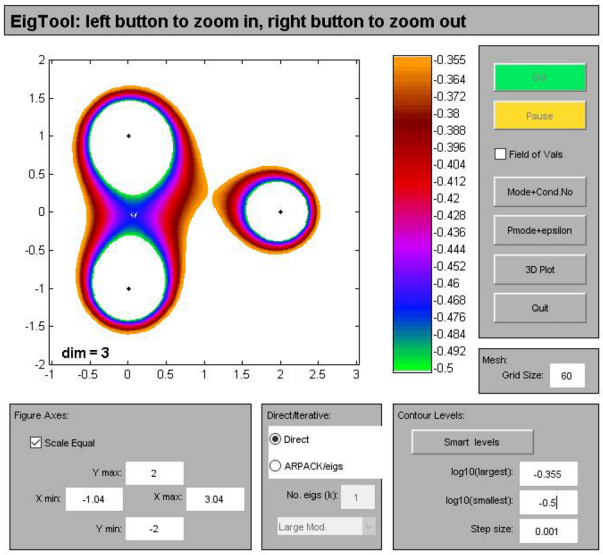

Figure 15: Pseudospectra of matrix C (with $r = 0$) from Example 2.5.

sensitivity of matrix eigenvalues. Research on pseudospectra has been extensive over the last 30 years; see [11] for a good survey of results and applications.

By varying ε in the same way that we have varied r in our approach, we see similar behaviors between eigenvalue orbits and the boundaries of pseudospectra. As an example, one can compare the discussion in [1], page 275, to our analysis of eigenvalue orbits in Section 3.2. The authors note that for sufficiently small values of ε, the boundary of $\Lambda_\varepsilon(A)$ consists of disjoint curves around each eigenvalue. As ε grows, so do the boundaries, and eventually they will begin to coalesce with each other. Analogously, for r sufficiently small, an eigenvalue orbit consists of disjoint curves around each eigenvalue. We can increase r until two components of an orbit intersect at a singularity.

Figure 15 shows some pseudospectra of matrix C (with $r = 0$) from Example 2.5. We can see the pseudospectral boundaries coalescing for certain values of ε. The figure was created using Eigtool, the Matlab software by Tom Wright which is freely available at the Pseudospectra Gateway [14]

Using the fact that the boundaries of $\Lambda_\varepsilon(A)$ are algebraic curves, the authors in [1] prove that if two components of $\Lambda_\varepsilon(A)$ coalesce at z_0, then z_0 is a multiple eigenvalue of a matrix A' such that $\|A - A'\| = \varepsilon$. This result is reminiscent of Theorem 3.2 which states that orbit singularities correspond to multiple eigenvalues. Are there other connections between these two families of algebraic curves, namely the boundaries of $\Lambda_\varepsilon(A)$ and eigenvalue orbits?

REFERENCES

[1] R. Alam and S. Bora. On sensitivity of eigenvalues and eigendecompositions of matrices. *Linear Algebra Appl.*, 396:273–301, 2005.
[2] L. Cvetkovic and V. Kostic. Between Geršgorin and minimal Geršgorin sets. *J. Computat. Appl. Math.*, 196:452–458, 2006.
[3] L. Cvetkovic, V. Kostic, and R.S. Varga. A New Geršgorin-type eigenvalue inclusion set. *Electron. Trans. Numer. Anal.*, 18:73–80, 2004.

Electronic Journal of Linear Algebra, ISSN 1081-3810
A publication of the International Linear Algebra Society
Volume 38, pp. 227-253, March 2022.

[4] R.A. Horn and C.R. Johnson. *Topics in Matrix Analysis*. Cambridge University Press, Cambridge, 1991.
[5] C.R. Johnson. Numerical determination of the field of values of a general complex matrix. *SIAM J. Numer. Anal.*, 15:595–602, 1978.
[6] K. Kendig. *A Guide to Plane Algebraic Curves*, MAA Dolciani Mathematical Expositions 46(7). The Mathematical Association of America, Washington DC, 2011.
[7] R. Kippenhahn. Über den Wertevorrat einer Matrix. *Math. Nachr.*, 6:193–228, 1951.
[8] J.C. Langer and D.A. Singer. Foci and foliations of real algebraic curves. *Milan J. Math.,* 75:225–271, 2007.
[9] J.C. Langer and D.A. Singer. Reflections on the lemniscate of Bernoulli: The forty eight faces of a mathematical gem. *Milan J. Math.,* 78:643–682, 2010.
[10] E.A. Rice. On the foci of plane algebraic curves with applications to symmetric cubic curves. *Amer. Math. Monthly*, 43:10, 618–630, 1936.
[11] L.N. Trefethen and M. Embree. *Spectra and Pseudospectra*, Princeton University Press, Princeton, NJ, 2005.
[12] R.S. Varga. *Geršgorin and His Circles*. Springer Series in Computational Mathematics 36. Springer-Verlag, Berlin, 2004.
[13] C.W. Wampler. The geometry of singular foci of planar linkages. *Mech. Mach. Theory,* 39(11):1123–1138, 2004.
[14] T.G. Wright. EigTool, 2002. http://www.comlab.ox.ac.uk/pseudospectra/eigtool/
[15] A.D. Wunsch. *Complex Variables with Applications*. Addison Wesley, 1994.
[16] P.F. Zachlin and M.E. Hochstenbach. On the field of values of a matrix. *Linear Multilinear Algebra*, 56:185–225, 2008. English translation with comments and corrections of [7].